The 2010 IEEE/RSJ International Conference on
Intelligent Robots and Systems
October 18-22, 2010, Taipei, Taiwan

Control of a Multiple Sections Flexible Endoscopic System

Bérengère Bardou*†, Philippe Zanne, Florent Nageotte and Michel de Mathelin
LSIIT laboratory - University of Strasbourg, CNRS - France

Abstract— **The use of flexible endoscopes in new surgical procedures such as NOTES, i.e. Natural Orifice Transluminal Endoscopic Surgery, raises many problems. Indeed, the movements of conventional flexible endoscopes are limited and surgeons can only perform basic tasks with these systems. In order to enhance endoscope possibilities and workspace, we are currently developing a robotized system. The prototype we propose is based on the combination of several flexible endoscopes. The kinematic model of the system is detailed in order to develop a method of control. The paper presents the implementation of a control strategy using an external sensor which allows to deal with non linearities induced by the cable mechanism of the endoscopes.**

I. Introduction

Flexible endoscopes have been recently used to perform a new kind of surgical procedure called NOTES, i.e. Natural Orifice Transluminal Endoscopic Surgery. More than 20 operations have already been performed on human beings in Strasbourg [1]. However, conventional endoscopes are inadequate for carrying out complex transluminal surgical tasks. Nonetheless flexible endoscopes are a good basis for developing more complex systems, because they are widely used and allow to overcome several difficult medical constraints such as asepsis. A first robotized system has been proposed in [2]. The chosen design for our new experimental prototype consists of a video endoscope and two articulated arms. These arms are attached to the endoscope and provide additional degrees of freedom to the system as well as triangulation of the surgical instruments which can translate and rotate inside each arm. All degrees of freedom are motorized. In this prototype, the instrument motion is teleoperated using two master interfaces.

Given the high number of degrees of freedom, it was important to establish a kinematic model of the prototype in order to predict the shape and the position of each arm and the position of the surgical instruments in function of the motor positions. The model used in this paper is inspired by continuum robot modeling from [3]. This paper presents the control strategy for controlling the instrument using all the degrees of freedom of the system.

The paper is organized as follows. The following section describes our robotized prototype and the modeling details used to control the system. The third section presents the experimental setup and the characterization of the kinematic model. Finally, the last section provides experimental results of the position control of the system.

*This work has been supported by the Alsace Region council.
‡This work has been funded by the french ministry of economy and finance through the Anubis project.
†Authors wish to thank Karl Storz Endoskope GmbH for their support and the IRCAD for the facilities and medical advices.

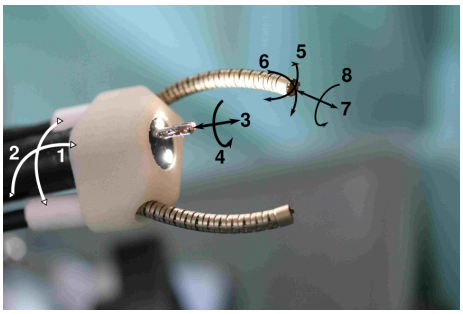

Fig. 1. Tip of the prototype and DOFs of the system: (1-2) orientation of the main endoscope equipped with the endoscopic camera, (3-4) translation and orientation of instruments inside the channel of the endoscope, (5-6) orientation of one arm, (7-8) translation and orientation of the instrument inside one arm

II. Endoscopic prototype

A. Motorization of the system

The slave system has been developed in collaboration with Karl Storz[1] based on a manual endoscopic system. Our prototype consists of a classical endoscope (12mm diameter) and two flexible hollow arms (4mm diameter) which are attached to the endoscope. This endoscope provides two additional working channels for conventional instruments. The hollow arms are fixed on the circumference at the end-part of the bending tip of the endoscope using a specific cap. This cap also allows to deflect the arms from the main direction of the endoscope. This provides triangulation between the arms and the endoscopic view and it enhances the cooperation area of the two arms. A view of the tip of the prototype is presented on fig.1. This prototype has been developed as a laboratory experimental system but it is not intended to be used in vivo. We are currently developing a new robotic endoscopic system similar in principle to the one presented which will be adapted to in vivo constraints.

The endoscope segment and the arm segments are not coupled by cable routing but they are constrained by the end cap. The orientation of the main endoscope as well as the orientation of both arms are driven by cables which are rolled up around pulleys. The pulleys are controlled by rotary motors mounted on the endoscope and the arms handles (see fig.3). So as to choose a solution for the motorization, the

[1]Karl Storz Endoskope GmbH, Germany

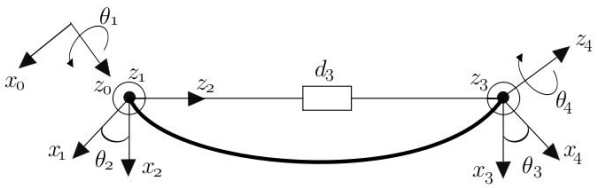

Fig. 2. Modeling of a flexible and continuum section

	θ_i	d_i	α_i	a_i
$0-1$	θ_1	0	$-\frac{\pi}{2}$	0
$1-2$	θ_2	0	$\frac{\pi}{2}$	0
$2-3$	0	d_3	$-\frac{\pi}{2}$	0
$3-4$	θ_4	0	$\frac{\pi}{2}$	0
$4-5$	θ_5	0	0	0

TABLE I

DH TABLE OF A FLEXIBLE SECTION

torques required to bend the tip of the main endoscope and the arms have been estimated without load.

The instruments are translated into the arms thanks to linear motors. Moreover, a rotary motor can be mounted onto the translation unit so as to rotate the surgical instruments around their own axis.

Overall, the whole system can have up to 12 actuated DOFs (see fig.1) which can be combined in several manners and can hence provide solutions to many medical procedures. More details on the robotization of the system are presented in [4].

B. Modeling of the system

1) Position kinematic modeling: The bending parts of the endoscope and the arms can be considered as "continuum robots". An interesting modeling of this kind of robot consists in representing the flexible bending parts as a system composed of rigid links. Under the assumptions that the continuum section is inextensible and has constant curvature and that the wires are equally spaced around the bending section circumference, a continuum robot can be modeled thanks to discrete joints as described on fig.2. Thus Denavit-Hartenberg (DH) conventions can be used, but with interdependent DH parameters.

The reference frame is positionned so that z-axis is along the backbone of the flexible section and x-axis points toward one of the pull-wires (see fig.5). This modeling can be used for the endoscope bending tip as well as for the arms representation.

One notes k the curvature of the endoscope bending section, L the length of this section and φ the orientation of the bending plane. k_B, φ_B and L_B (resp. k_C, φ_C and L_C) refer to the same parameters for the arm B (resp. arm C). The DH parameters can be linked to these geometric parameters

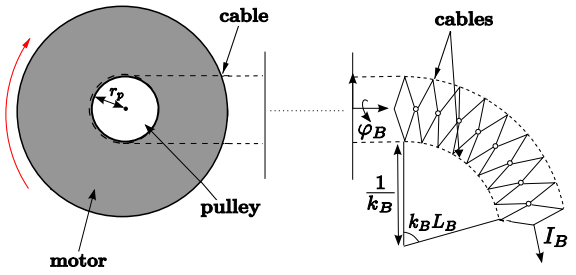

Fig. 3. Model of the deflection of armB in response to the variation of cable length

of the flexible section thanks to the following relations (f_1):

$$\theta_1 = \varphi \qquad \theta_2 = \theta_4 = \theta = \frac{kL}{2} \tag{1}$$

$$d_3 = \frac{2}{k} * sin(\theta) \tag{2}$$

$$\theta_5 = -\varphi \tag{3}$$

$$\theta_{1i} = \varphi_i \qquad \theta_{2i} = \frac{k_i L_i}{2} \tag{4}$$

$$d_{3i} = \frac{2}{k_i} * sin(\theta_{2i}) \tag{5}$$

$$\theta_{5i} = -\varphi_i \qquad \text{with} \qquad i \in \{B,C\}. \tag{6}$$

To these geometric parameters one must add I_B (resp. I_C) which is the translation of the instruments into the hollow arms. All these geometric parameters are illustrated by fig.3. Since we will only take interest in the instrument positioning, not its orientation, it is not necessary to introduce the instrument rotation in the model.

One can notice that $k = 0$ is a singular configuration where d are no longer defined. This position corresponds to a "straight" configuration of the flexible section and can be solved using a second order Taylor approximation.

The angle φ and the curvature k can be related to the length distribution of the two wires ΔL_1 and ΔL_2 by the following equations (f_2):

$$k = \frac{\sqrt{\Delta L_1^2 + \Delta L_2^2}}{Lr} \tag{7}$$

$$\varphi = atan2(\Delta L_2, \Delta L_1) \tag{8}$$

where r is the endoscope radius. Identical equations are valid for the arms:

$$k_i = \frac{\sqrt{\Delta L_{1i}^2 + \Delta L_{2i}^2}}{L_i r_i} \tag{9}$$

$$\varphi_i = atan2(\Delta L_{2i}, \Delta L_{1i}) \qquad \text{with} \qquad i \in \{B,C\} \tag{10}$$

where r_i is the arm radius.

Finally the relation between the length modification of the cables and the actuator positions $q = [q_1, q_2, q_{1B}, q_{2B}, q_{1C}, q_{2C}]^T$ is given by (f_3):

$$\Delta L_i = R_p * \Delta q_i \tag{11}$$

$$\Delta L_{ij} = r_p * \Delta q_{ij} \tag{12}$$

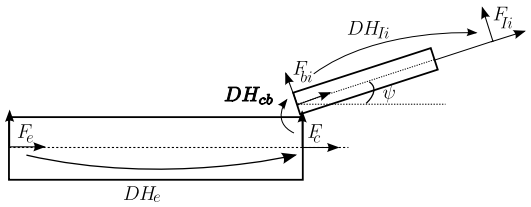

Fig. 4. Side view of the system with one arm. ψ is the deflection angle provided by the end cap

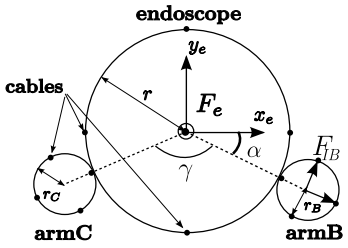

Fig. 5. Top view of the basis of the system

$$\text{with} \qquad i \in \{1,2\} \qquad \text{and} \qquad j \in \{B,C\}$$

where R_p and r_p are respectively the radius of the endoscope pulleys and of the arms pulleys.

The relative position and orientation of the arms with respect to the endoscope is defined by three angles: α is the angle between arm B and Ox axis of the reference frame, γ is the angle between both arms. These angles are represented on fig.5. In order to enhance the surgical workspace and to provide triangulation, i.e. a configuration similar to open surgery or laparoscopy, an end cap is fixed on the rigid section of the endoscope. It deflects the arms and their tools of an angle ψ from the endoscope main direction. These parameters, determined by the design of the system, introduce a new transformation: $\mathbf{DH_{cb}}$. The complete system is a tree-like robot with two end effectors. This means that both arms have a common kinematic chain. The entire geometric model i.e. instrument position $\mathbf{X_{eI}}$ in the endoscope basis frame F_e, is obtained by chaining together the geometric models of the flexible sections as on fig.4:

$$(\Delta q, \Delta q_i) \xrightarrow{f_3} (\Delta L, \Delta L_i) \xrightarrow{f_2} (\phi, k, \phi_i, k_i) \xrightarrow{f_1} (\theta, d, \theta_i, d_i) \xrightarrow{M} X_{eI} \tag{13}$$

$$M = DH_e * DH_{cb} * DH_{Ii}. \tag{14}$$

where $\mathbf{DH_e}$ is the Denavit-Hartenberg matrix of the endoscope and $\mathbf{DH_{Ii}}$ the transformation from the instrument basis to the instrument extremity.

2) Velocity kinematic modeling: The velocity kinematics can be written as :

$$\dot{X} = J(q)\dot{q}, \tag{15}$$

where $\mathbf{X}$ is the task space vector, i.e. position of one or two end effectors and $\mathbf{q}$ the joint positions vector. The matrix $\mathbf{J}$ is the jacobian and is a function of joint variables $\mathbf{q}$. For our prototype:

$$q = [q_1, q_2, q_{1B}, q_{2B}, I_B, q_{1C}, q_{2C}, I_C]^T, \tag{16}$$

and $\mathbf{X}$ is defined depending on the task the user wants to perform. Because of non linearities in functions f_1, f_2 and f_3 the jacobian matrix results in long elements and its expression is omitted here due to limited space. But the procedure for obtaining it is quite straightforward. The numerical computation of the matrix is relatively simple and can be easily implemented. Following the same approach as in [5], the forward velocity kinematic of an instrument can be computed as a series of jacobian matrices:

$$(\dot{\Delta q}, \dot{\Delta q_i}) \xrightarrow{J_3} (\dot{\Delta L}, \dot{\Delta L_i}) \xrightarrow{J_2} (\dot{\phi}, \dot{k}, \dot{\phi_i}, \dot{k_i}) \xrightarrow{J_1} (\dot{\theta}, \dot{d}, \dot{\theta_i}, \dot{d_i}) \xrightarrow{J} \dot{X_{eI}} \tag{17}$$

In the following sections we focus on the position of a single instrument and only one arm (armB) of the prototype is used.

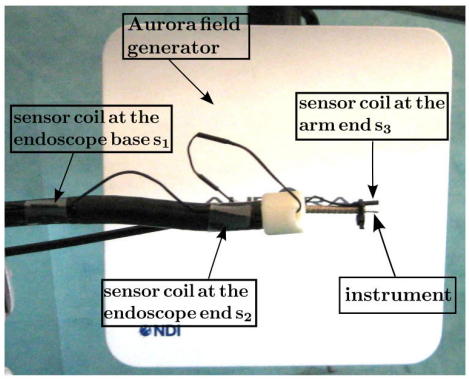

Fig. 6. Experimental setup

III. Assessment of the kinematic model

Experiments have been carried out on the prototype in order to assess the validity of the kinematic model proposed in section II. For this purpose, an external sensor, namely the Aurora electromagnetic system from NDI, has been used to measure the movements of the instrument. [6] and [7] propose similar approaches with steerable catheters.

A. Experimental setup

The Aurora provides the position and orientation (5DOFs) of small sensor coils expressed in the Aurora reference frame. In the following experiments, two sensor coils were attached to both extremities of the bending section of the endoscope ($S1$ at the basis and $S2$ at the tip). Because of the size of the sensor coils, it was not possible to directly attach one to the instrument. Instead, one sensor coil $S3$ was attached at the tip of the arm and it was oriented along the direction of motion of the instrument. The experimental setup is shown on fig.6. The cartesian position of the instrument in the endoscope basis frame is obtained as explained in the following section.

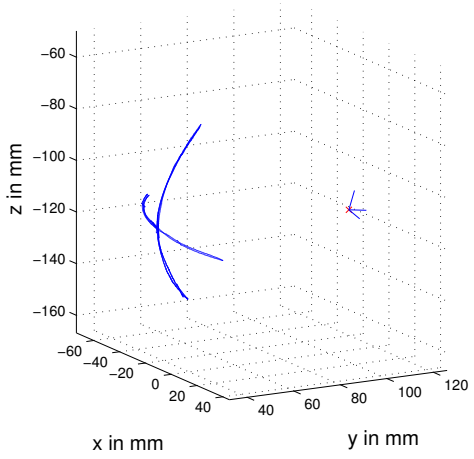

Fig. 7. Determination of the endoscope basis frame

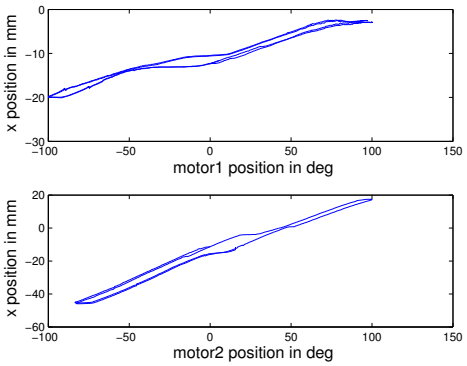

Fig. 8. Endoscope backlash

B. Computation of the position of the instrument

There are two main problems for obtaining the position of the tip of the instrument expressed in the endoscope basis frame : first determining the orientation of the endoscope basis frame with respect to the Aurora frame and second obtaining the position of the instrument from the position and orientation of the sensor coil $S3$ at the tip of the arm.

1) Transformation between Aurora and endoscope frames: The sensor at the basis of the endoscope $S1$ allows to measure the translation from the Aurora frame to the endoscope frame which will be denoted O_{0E}. However, the relative orientation cannot be directly obtained from the sensor coil because it is oriented along the main endoscope axis. For this purpose, one analyzes the motion of the endoscope along the two main directions. The endoscope is first positioned in a "straight" configuration. This position can be automatically detected since it maximizes the distance between sensor $S1$ and sensor $S2$. Then the endoscope is actuated using back and forth motions along both main directions by activating only one motor at each time. Two planes Π_1 with normal n_1 and Π_2 with normal n_2 are then fitted on the measured positions.

By convention, the x-axis for the endoscope basis frame has been chosen to point towards cable 1 (see fig. 5) so that it corresponds to a positive movement of the first motor. The z-axis is computed as the result of the cross product $n_1 \wedge n_2$. Finally, for obtaining an orthogonal matrix for the rotation, the transformation from the Aurora frame to the endoscope frame, $\mathbf{M_{0E}}$, is given by:

$$M_{0E} = \begin{pmatrix} n_2 & z \wedge n_2 & z & O_{0E} \\ 0 & 0 & 0 & 1 \end{pmatrix}$$

The motions used for determining the orientation of the frame are illustrated on fig.7.

2) Position and orientation of the instrument: Thanks to the previous calibration step and using the sensor coil $S3$, one can obtain the cartesian position of the tip of the arm in the endoscope basis frame :

$$ES3 = M_{0E}^{-1} S3.$$

The direction of the instrument in the aurora frame is provided by the orientation of sensor $S3$ $\mathbf{R_{0S3}}$. It can easily be obtained in the frame of the endoscope using

$$R_{ES3} = R_{0E}^T R_{0S3}.$$

The missing information is the distance I_B between sensor $S3$ and the tip of the instrument. The translation of the instrument in the arm is directly controlled using a linear motor. Since this DOF is completely decoupled from the others and directly driven, it is possible to accurately estimate the motion of the tip of the instrument by measuring the motion of the linear motor. The origin of the translation (i.e. $I_B = I_{B0}$) is obtained by initially bringing the axis to its stop. Finally, the transformation between the endoscope frame and the tip of the instrument is computed as :

$$M_{EI} = \begin{pmatrix} R_{ES3} & ES3 + R_{ES3} \begin{pmatrix} 0 \\ 0 \\ I_B \end{pmatrix} \\ 0 & 1 \end{pmatrix}$$

C. Displaying non linearities

Before achieving control, we must characterize the different section movements. The end position of each flexible section was measured in response to variations in joint parameters. The comparison between the cartesian movements and the motors measurements revealed strong non linearities. The wire transmission between the motors and the bending section induces friction and backlash. Indeed cable tension is not warranted inside the flexible shaft when the bending part is "straight" or during back-and-forth movements. The results are presented on fig.8 for the endoscope and fig.9 for the arm. One can notice a deadband at each change of direction of the motors but also when bending sections are passing through the straight configuration as described earlier. Furthermore, the deadband of this backlash depends on the section configuration before the displacement but also on the unknown shape of the flexible shaft.

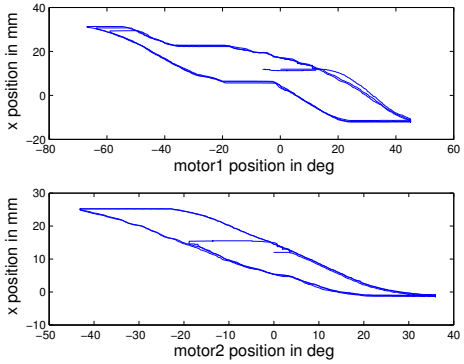

Fig. 9. Arm backlash

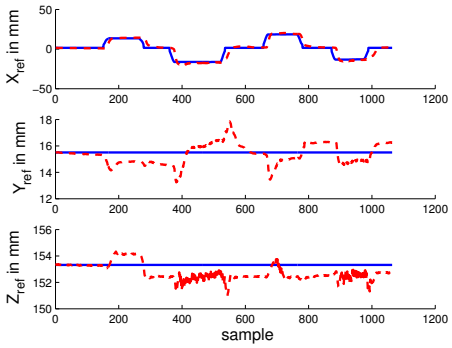

Fig. 11. Results of the control on x-axis

In view of these non linearities, it seems difficult to correctly control the cartesian position of the instrument without any external sensor and feedback. Other possibilities could be to redesign the entire endoscopic system, such as [8], [9] or [10], or to use independant actuators to take up the antagonistic slack [11]. Since we chose to work with existing and marketed endoscopic systems, both solutions are not satisfying.

IV. Control of the system using an external sensor

From the previous results, it seems that the system should be controlled in closed loop using an external sensor. We tried to use the Aurora as the external sensor. Several sets of experiments were carried out. We only considered two flexible sections: the endoscope and one arm. Five degrees of freedom are controlled: 2 for each bending part and one for the instrument translation. The sensor coils are attached to the system as discussed in the previous section.

The model of the control loop is given on fig.10. The cartesian position of the instrument in the endoscope basis frame is teleoperated from an Omega interface[2]. The master displacement is provided by the interface as $\Delta\mathbf{X_{int}}$. Consequently $\mathbf{X_{ref}}$ is the suited cartesian position resulting from a cartesian displacement of $\Delta\mathbf{X_{int}}$ from an initial position $\mathbf{X_0}$:

$$X_{ref} = X_0 + \Delta X_{int}.$$

[2]Force Dimension, Switzerland

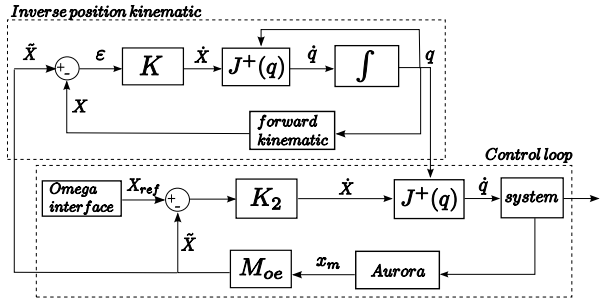

Fig. 10. Block diagram of the control loop

Since $\mathbf{X_{ref}}$ is expressed in the endoscope frame and the Aurora provides information in its own frame, the transformation $\mathbf{M_{oe}}$ is required for controlling the system, as shown on fig.10. It is obtained from a calibration step described in the previous section. $\tilde{\mathbf{X}}$ is the estimate of the position of the instrument in the reference frame.

All motors are velocity controlled at low-level with external position loops running at 2000Hz on a unique controller. The magnetic sensor is synchronized with the control loop at 25 Hz. The jacobian matrix computation was detailed in section II. For a given vector $\dot{\mathbf{X}} = [\dot{x}, \dot{y}, \dot{z}]^T$ defining the desired velocity in the task space, the joint velocity to be applied can be computed as:

$$\dot{q} = J^+(q)\dot{X}, \tag{18}$$

where $\mathbf{J}^+$ is the Moore-Penrose jacobian pseudo inverse given by :

$$J^+ = J^T(JJ^T)^{-1}. \tag{19}$$

With this computation, the obtained velocity is the one ensuring the desired operational velocity with minimum norm. However one cannot use the measured joint positions for computing $\mathbf{J}^+(\mathbf{q})$. Indeed backlash induce important errors in the estimation of the cartesian position which leads to large errors in the jacobian and to instability. Thus the second loop computes the theoretical motor configuration corresponding to the cartesian motion measured by Aurora system (see fig.10). Analytic solution of inverse kinematic presented in [12] cannot be applied here because of rigid sections introduced by the instrument translation and the rigid tip of the endoscope. The second loop numericaly computes the inverse kinematic solution. In a first approach, we used a simple proportional controller K_2 for the main closed loop. Since the system includes an integrator, this is sufficient to cancel the static error.

We performed one experiment for each axis and another one for the full movement. The master interface offers a motion range of 16cm on each axis. The results presented on fig.11 and fig.12 only refer to experiments on x-axis and on a full 3D trajectory due to limited space.

In the experiment of fig.11, we only applied a movement on the x-axis of *Fe* while we maintained positions on y

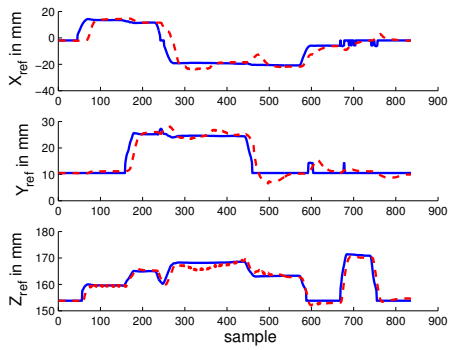

Fig. 12. Results of the control of the full motion

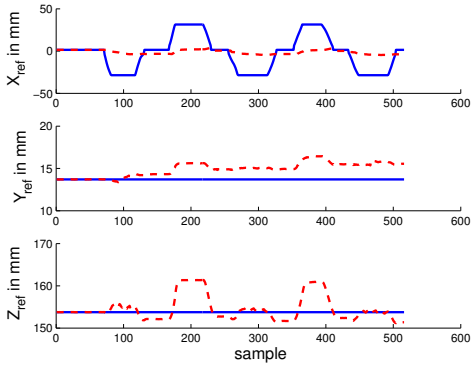

Fig. 13. Results of the open loop control on x-axis

and z-axis. The dash line represents the instrument position measured by Aurora system and expressed in the reference frame and the solid line is the reference. One can notice that the measured position converges to the desired position. The curves of fig.12 exposed the results of a full motion along x, y or z-axis. For these sets of experiments the average error of the tracking trajectory does not exceed 4mm.

As a comparison we made the same experiments but with an open loop control using the kinematic model. Our assumption on the necessity to add an external sensor is confirmed by the results of fig.13 and fig.14. The graphics show displacement of the flexible sections of only few millimeters while the instrument should move several centimeters. Moreover small errors on the identification of the kinematic parameters induce small motions on other axes. Therefore the effective position does not correspond to the desired position and the average error of the tracking trajectory exceeds 15mm.

V. Conclusion

The flexible nature of endoscopes presents interesting problems in terms of robotic control. But the presence of important backlash induced by the cable transmission makes it challenging. Controlling the instrument position with only the kinematic model proved to be inaccurate and difficult. Therefore we proposed to add an external sensor, the Aurora magnetic measurement system, to provide feedback. Experiments show that the system can be teleoperated even with small inaccuracies on the kinematic model and large non linearities. This paper proposed a solution to control a flexible and cable-driven endoscopic system. A more advanced controller would allow to enlarge the bandwith and to obtain best results. Another interesting strategy would be to only use visual feedback from the embedded camera of the endoscope.

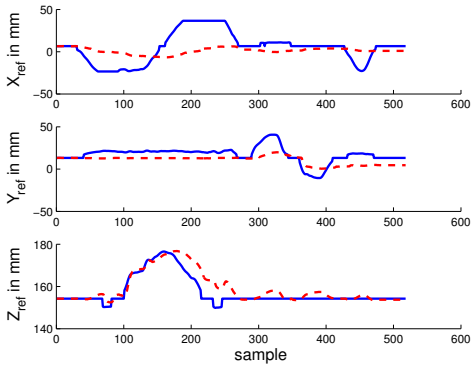

Fig. 14. Results of the open loop control of the full motion

References

[1] J. Marescaux, B. Dallemagne, S. Perretta, A. Wattiez, D. Mutter, and D. Coumaros, "Surgery without scars: report of transluminal cholecystectomy in a human being," *Arch Surg*, vol. 142, pp. 823–826, 2007.

[2] L. Ott, P. Zanne, F. Nageotte, and M. de Mathelin, "Physiological motion rejection in flexible endoscopy using visual servoing," in *IEEE Int. Conf. on robotic and automation*, 2008.

[3] M. Hannan and I. Walker, "Kinematics and the implementation of an elephant's trunk manipulator and other continuum style robots," *Journal of Robotic Systems*, vol. 20, no. 2, pp. 45–63, 2003.

[4] B. Bardou, F. Nageotte, P. Zanne, and M. de Mathelin, "Design of a telemanipulated system for transluminal surgery," in *IEEE Int. Conf. on Engineering in Medicine and Biology*, 2009.

[5] B. Jones and I. Walker, "A new approach to jacobian formulation for a class of multi-section continuum robots," in *IEEE Int. Conf. on robotic and automation*, Barcelona, April 2005.

[6] Y. Ganji and F. Janabi-Sharifi, "Catheter kinematics for intracardiac navigation," *IEEE Transactions on Biomedical Engineering*, vol. 56, no. 3, pp. 621–632, March 2009.

[7] D. B. Camarillo, C. R. Carlson, and J. K. Salisbury, "Configuration tracking for continuum manipulators with coupled tendon drive," *IEEE Transactions on Robotics*, vol. 25, no. 4, pp. 798–808, August 2009.

[8] D. J. Abbott, C. Becke, R. I. Rothstein, and W. J. Peine, "Design of an endoluminal notes robotic system," in *IEEE Int. Conf. on Intelligent Robots and Systems*, San diego, October 2007.

[9] S. Naoki, S. Kazuki, H. Asaki, I. Keiichi, M. Edwardo, S. Shigeyuki, H. Mitsuhiro, O. Yoshito, and T. Hisao, "Development of an endoscopic robotic system with two hands for various gastric tube surgeries," *Studies in Health technology and informatics*, vol. 94, pp. 349–53, 2003.

[10] Z. Thant, S. Low, S. Tang, and L. Phee, "Ergonomic master controller for flexible endoscopic gastrointestinal robot manipulator," in *Int. Conf. on Biomedical and Pharmaceutical Engineering*, 2006.

[11] S. C. Jacobsen, H. Ko, E. K. Iversen, and C. C. Davis, "Control strategies for tendon-driven manipulators," in *IEEE Int. Conf. on Robotic and Automation*, 1989.

[12] S. Neppalli, M. A. Csencsits, B. A. Jones, and I. Walker, "A geometrical approach to inverse kinematics for continuum manipulators," in *IEEE International Conference on Intelligent Robots and Systems*, 2008.